Impact of Nuclear Quantum Effects on the Molecular Structure of Bihalides and the Hydrogen Fluoride Dimer

Chet Swalina and Sharon Hammes-Schiffer*

Department of Chemistry, 104 Chemistry Building, The Pennsylvania State University, University Park, Pennsylvania 16802

Received: June 29, 2005; In Final Form: September 2, 2005

The structural impact of nuclear quantum effects is investigated for a set of bihalides, $[XHX]^-$, X = F, Cl, and Br, and the hydrogen fluoride dimer. Structures are calculated with the vibrational self-consistent-field (VSCF) method, the second-order vibrational perturbation theory method (VPT2), and the nuclear-electronic orbital (NEO) approach. In the VSCF and VPT2 methods, the vibrationally averaged geometries are calculated for the Born-Oppenheimer electronic potential energy surface. In the NEO approach, the hydrogen nuclei are treated quantum mechanically on the same level as the electrons, and mixed nuclear-electronic wave functions are calculated variationally with molecular orbital methods. Electron-electron and electron-proton dynamical correlation effects are included in the NEO approach using second-order perturbation theory (NEO-MP2). The nuclear quantum effects are found to alter the distances between the heavy atoms by 0.02−0.05 Å for the systems studied. These effects are of similar magnitude as the electron correlation effects. For the bihalides, inclusion of the nuclear quantum effects with the NEO-MP2 or the VSCF method increases the X−X distance. The bihalide X−X distances are similar for both methods and are consistent with two-dimensional grid calculations and experimental values, thereby validating the use of the computationally efficient NEO-MP2 method for these types of systems. For the hydrogen fluoride dimer, inclusion of nuclear quantum effects decreases the F−F distance with the NEO-MP2 method and increases the F−F distance with the VSCF and VPT2 methods. The VPT2 F−F distances for the hydrogen fluoride dimer and the deuterated form are consistent with the experimentally determined values. The NEO-MP2 F−F distance is in excellent agreement with the distance obtained experimentally for a model that removes the large amplitude bending motions. The analysis of these calculations provides insight into the significance of electron-electron and electron-proton correlation, anharmonicity of the vibrational modes, and nonadiabatic effects for hydrogen-bonded systems.

I. Introduction

Hydrogen bonding plays an important role in biomolecular structure and function,[1] molecular self-assembly,[2] and solvation.[3] Theoretical studies of hydrogen-bonded systems are challenging due to the low-frequency, anharmonic intermolecular vibrations.[4,5] Moreover, nuclear quantum effects of the hydrogen atom motions significantly impact the structures and spectroscopic properties of these systems. Conventional molecular dynamics and electronic structure calculations of hydrogen-bonded systems typically neglect the nuclear quantum effects.

Recently, the role of nuclear quantum effects in hydrogen-bonded systems has been investigated with a variety of theoretical methods. The quantum diffusion Monte Carlo approach has been used to study the impact of nuclear quantum effects on donor-acceptor distances, rotational constants, and hydrogen bond energies in gas-phase hydrogen-bonded clusters.[5−7] A disadvantage of the quantum diffusion Monte Carlo method is that it requires analytical potentials to describe the potential energy surfaces of larger systems. The vibrational self-consistent-field (VSCF),[8,9] the multimode vibrational configuration interaction,[5,10] and the second-order vibrational perturbation theory (VPT2)[11,12] approaches have been used to investigate anharmonic effects on frequencies and interaction energies in hydrogen-bonded systems. Although these methods can utilize ab initio potential energy surfaces, they are computationally demanding for larger systems. Path integral methods have been applied to study hydrogen bonding in solution. For example, the Car-Parrinello molecular dynamics approach combined with a path integral treatment of the nuclei[13] has been used to analyze the structural impact of nuclear quantum effects on hydrogen bonding in liquid hydrogen fluoride and water.[14,15]

The nuclear-electronic orbital (NEO) method is an alternative approach for including nuclear quantum effects directly into electronic structure calculations.[16−22] In the NEO approach, selected nuclei are treated quantum mechanically on the same footing as the electrons, and mixed nuclear-electronic wave functions are calculated variationally using molecular orbital techniques. Both the nuclear and the electronic wave functions are expanded in terms of Gaussian basis functions. The nuclear basis set typically includes *s*, *p*, and *d*-type Gaussians. In the NEO treatment of hydrogen-bonded systems, only the hydrogen nuclei are treated quantum mechanically. Dynamical electron-electron and electron-proton correlation effects are included in the NEO framework using second-order perturbation theory (NEO-MP2).[20] Other groups[23−26] have also studied hydrogen bonded systems using a related nuclear molecular orbital method, but their studies used only a single 1*s* basis function for the hydrogen nucleus and did not include electron-electron or electron-nuclear correlation.

* Corresponding author: E-mail: shs@chem.psu.edu.

10.1021/jp053552i CCC: $30.25
Published on Web 10/19/2005

The NEO method possesses several advantages over other methods for including nuclear quantum effects. Anharmonic properties of the potential energy surface are included directly in NEO calculations. Moreover, the impact of nuclear quantum effects on the electronic wave function is inherently included in NEO calculations because the nuclear and electronic wave functions are calculated simultaneously. This type of response is not fully included in methods that calculate nuclear wave functions on Born-Oppenheimer electronic potential energy surfaces with no feedback between the nuclear and electronic wave functions. In addition, the NEO approach is more computationally efficient for the calculation of vibrationally averaged molecular structures than the grid-based methods such as VSCF and the VPT2 method. NEO calculations at the Hartree-Fock (NEO-HF) or second-order perturbation theory (NEO-MP2) levels are approximately as expensive as the corresponding conventional RHF or MP2 analogues.

In this paper, we utilize three different approaches to study the impact of nuclear quantum effects on molecular structure. The NEO-MP2 and VSCF approaches are applied to a set of bihalide compounds, $[XHX]^{-1}$ (X = F, Cl, Br), and the NEO-MP2, VSCF, and VPT2 approaches are applied to the hydrogen fluoride dimer, $(HF)_2$. Our objective is to compare the geometries calculated with a variety of quantum mechanical approaches to available experimental data. Additionally, we analyze the significance of electron-electron and electron-proton correlation, anharmonicity of the vibrational modes, and nonadiabatic effects for these hydrogen-bonded systems. Bihalides exhibit anharmonic potential energy surfaces that must be described accurately to recover vibrationally averaged molecular properties. Experimental bond lengths and frequencies are available for the bihalides with fluorine and chlorine. These bihalide systems have also been studied by Del Bene and Jordan using a two-dimensional grid-based approach.[27] The hydrogen fluoride dimer exhibits an asymmetric hydrogen bond that strongly influences vibrationally averaged molecular properties. Experimental F−F distances are available for the hydrogen fluoride dimer and the deuterated form of the dimer.[28,29]

The remainder of the paper is organized as follows. Section II provides a summary of the NEO-HF, NEO-MP2, VSCF, and VPT2 methods. Section III presents the results for the bihalides and the hydrogen fluoride dimer. The final section presents conclusions and future directions.

II. Theory and Methods

A. Nuclear-Electronic Orbital Method. In the NEO approach, the system is divided into three parts: N_e electrons, N_p quantum nuclei, and N_c classical nuclei. The NEO-HF and NEO-MP2 approaches have been described in detail elsewhere.[16,20] At the Hartree-Fock level, the total nuclear-electronic wave function can be approximated as a product of single configurational electronic and nuclear wave functions:

$$\Psi_{tot}(\mathbf{r}^e,\mathbf{r}^p) = \Phi_0^e(\mathbf{r}^e)\Phi_0^p(\mathbf{r}^p) \quad (1)$$

where $\Phi_0^e(\mathbf{r}^e)$ and $\Phi_0^p(\mathbf{r}^p)$, respectively, are antisymmetrized wave functions (determinants of spin orbitals) representing the electrons and fermionic nuclei such as protons. (Here $\mathbf{r}^e$ and $\mathbf{r}^p$ denote the spatial coordinates of the electrons and quantum nuclei, respectively.) The spatial orbitals for the electrons and the quantum nuclei are expanded in Gaussian basis sets, and the variational method is used to minimize the total energy with respect to both the electronic and nuclear molecular orbitals.

The NEO-MP2 corrections for electron-electron, proton-proton, and electron-proton correlation are derived in ref 20. For a system with N_e paired electrons and N_p high spin quantum protons, the reference NEO-HF Hamiltonian is defined as

$$H_0^{NEO} = \sum_i^{N_e}\{h^e(i) + \nu_{ee}^{HF}(i) + \nu_{ep,e}^{HF}(i)\} + \sum_{i'}^{N_p}\{h^p(i') + \nu_{pp}^{HF}(i') + \nu_{ep,p}^{HF}(i')\} \quad (2)$$

The unprimed indices refer to electrons, and the primed indices refer to quantum protons. In eq 2, h^e and h^p are the one-particle terms for the electrons and protons, respectively, and are defined in ref 16. Morever, as defined in ref 20, $\nu_{ee}^{HF}(i)$ is the Coulomb-exchange operator for the electrons, $\nu_{ep,e}^{HF}(i)$ is the electron-proton Coulomb operator for the electrons, $\nu_{pp}^{HF}(i')$ is the Coulomb-exchange operator for the quantum protons, and $\nu_{ep,p}^{HF}(i')$ is the electron-proton Coulomb operator for the quantum protons. The combined perturbation for electron-electron and electron-proton correlation is $W = W_{ee} + W_{ep}$, where the perturbation for electron-electron correlation is defined as

$$W_{ee} = \sum_{i<j}^{N_e} r_{ij}^{-1} - \sum_i^{N_e} \nu_{ee}^{HF}(i) \quad (3)$$

and the perturbation for electron-proton correlation is defined as

$$W_{ep} = -\sum_i^{N_e}\sum_{i'}^{N_p} r_{ii'}^{-1} - \sum_i^{N_e} \nu_{ep,e}^{HF}(i) - \sum_{i'}^{N_p} \nu_{ep,p}^{HF}(i') \quad (4)$$

The total NEO-MP2 energy is $E^{NEO\text{-}MP2} = E^{NEO\text{-}HF} + E_{ee}^{(2)} + E_{ep}^{(2)}$, where

$$E_{ee}^{(2)} = \frac{1}{4}\sum_{abrs} \frac{|\langle ab|rs\rangle - \langle ab|sr\rangle|^2}{\epsilon_a^e + \epsilon_b^e - \epsilon_r^e - \epsilon_s^e} \quad (5)$$

$$E_{ep}^{(2)} = \sum_{aa'rr'} \frac{|\langle aa'|rr'\rangle|^2}{\epsilon_a^e + \epsilon_{a'}^p - \epsilon_r^e - \epsilon_{r'}^p} \quad (6)$$

Here a and b refer to occupied electronic molecular orbitals, and r and s refer to virtual electronic molecular orbitals. The indices a' and r', respectively, refer to occupied and virtual nuclear molecular orbitals. The energies ϵ_a^e and $\epsilon_{a'}^p$, respectively, are the electronic and nuclear orbital energies for the unperturbed Hamiltonian. Note that the MP2 corrections for electron-electron and electron-proton correlation are independent, thereby enabling two different types of NEO-MP2 calculations. One type of calculation includes only the correction for electron-electron correlation, NEO-MP2(ee), and the other type includes the corrections for both electron-electron and electron-proton correlation, NEO-MP2(ee+ep).

For the special case of systems with N_e paired electrons and a single quantum proton, the reference NEO-HF Hamiltonian is defined as

$$H_0^{NEO} = \sum_i^{N_e}\{h^e(i) + \nu_{ee}^{HF}(i) + \nu_{ep,e}^{HF}(i)\} + h^p(1') + \nu_{ep,p}^{HF}(1') \quad (7)$$

The advantages of this reference Hamiltonian over the conven-

tional reference Hamiltonian that includes the proton-proton Coulomb-exchange operator are discussed in ref 20. This reference Hamiltonian was used for the bihalide calculations in this paper.

The NEO methodology has been implemented in the GAMESS electronic structure program.[30] The DZSPDN hydrogen nuclear basis set was used for the NEO calculations presented in this paper. This DZSPDN nuclear basis set[16] includes two each of *s*-, *p*-, and *d*-type Gaussians, resulting in a total of 20 nuclear basis functions per hydrogen center. The aug′-cc-pVTZ electronic basis set,[31−33] in which the prime indicates that diffuse functions were placed only on the heavy atoms, was used for the bihalide calculations, and the aug-cc-pVTZ electronic basis set was used for the HF dimer calculations. At the NEO-HF level, analytical gradients[16] were used to carry out all geometry optimizations. Structures were identified as minima on the NEO potential energy surface by computing and diagonalizing the NEO Hessian matrix.[17] At the NEO-MP2 level, all geometry optimizations were performed using numerical gradients. A criteria of 10^{-5} hartree/Bohr was used for all geometry optimizations, and all SCF densities were converged to within 10^{-7}.

A significant source of error present in electronic structure calculations on hydrogen-bonded dimers is basis set superposition error (BSSE). BSSE is the mutual improvement of the electronic basis sets on the monomers in the overall basis of the dimer. Since BSSE can impact structures of hydrogen-bonded dimers,[34] we have estimated the magnitude of BSSE with the counterpoise correction[35] using both the NEO-MP2(ee+ep) and conventional MP2 methods for the HF dimer. Both the NEO and conventional counterpoise correction calculations were performed using the MP2/aug-cc-pVTZ optimized HF dimer geometry. The NEO-MP2(ee+ep) and conventional MP2 counterpoise corrections are −0.55 and −0.48 kcal/mol, respectively. Thus, the amount of BSSE is similar for the conventional MP2 and NEO-MP2 calculations.

B. VSCF and VPT2 Methods. The VSCF method as implemented by Chaban, Jung, and Gerber[8] was used to calculate vibrationally averaged geometries for the bihalides and the HF dimer. An option to calculate vibrationally averaged molecular structures within the VSCF framework is not implemented in the distributed version of GAMESS.[30] Therefore, we have incorporated this capability into an experimental version of the GAMESS code. At the VSCF level, the total molecular vibrational wave function is constructed as a product of vibrational normal mode wave functions. The expectation values of the Cartesian coordinates with respect to the VSCF ground-state wave function are determined through linear transformations. For all of the VSCF calculations, 16 directly computed quadrature points along each normal mode were used to construct the VSCF potential. The potentials were calculated at the MP2/aug′-cc-pVTZ level for the bihalides and at the MP2/aug-cc-pVTZ level for the HF dimer. Geometries obtained at the VSCF level and frequencies obtained at the VSCF and CC-VSCF levels[8] are reported. The CC-VSCF (correlation corrected VSCF) level includes a second-order perturbation theory correction to include dynamical correlation between the vibrational modes.

The VPT2 method as implemented by Barone[11] in the Gaussian03 package[36] was used to calculate vibrationally averaged geometries for the HF dimer at the MP2/aug-cc-pVTZ level. This method was not available for linear molecules such as the bihalides. In the VPT2 method, the zeroth-order vibrational wave functions are generated from the harmonic approximation, and the second-order perturbation theory corrections are calculated from the cubic force constants and semidiagonal quartic force constants. The required cubic and quartic force constants are obtained by numerical differentiation of the analytical Hessians. Vibrationally averaged molecular structures are standard output for VPT2 calculations in Gaussian03.[36]

TABLE 1: Experimental and Theoretical X−X Distances in Å for Bihalide Systems, $[XHX]^-$ with X = F, Cl, Br[a]

method	$[FHF]^-$ R_{FF}	$[ClHCl]^-$ R_{ClCl}	$[BrHBr]^-$ R_{BrBr}
experimental R_e	2.27771[b]	3.1122(26)[c]	N/A
experimental R_0	2.304[d]	3.14676(5)[c]	N/A
MP2	2.288	3.110	3.408
2D grid[e]	2.324	3.152	3.430
VSCF-MP2	2.311	3.131	3.424
NEO-MP2(ee)	2.321	3.150	3.449
NEO-MP2(ee)/1Dgrid	2.325	3.151	3.451
NEO-MP2(ee+ep)	2.313	3.139	3.437
NEO-MP2(ee+ep)/1Dgrid	2.318	3.142	3.440

[a] The aug′-cc-pVTZ electronic basis set and MP2 level of including electron-electron correlation were used in all calculations. The DZSPDN nuclear basis set was used in all of the NEO calculations. [b] Reference 38. [c] Reference 39. [d] Calculated using rigid rotor approximation and B_0 from ref 38. [e] Reference 27.

III. Results and Discussion

A. Bihalides. In this subsection, we analyze calculations for a set of $[XHX]^-$ systems with X = F, Cl, and Br. We compare the X−X distances obtained with the NEO approach to the distances obtained with two-dimensional grid methods by Del Bene and Jordan[27] and to distances obtained with the VSCF method. To enable this comparison, we used the aug′-cc-pVTZ electronic basis set and included electron-electron correlation at the MP2 level for all calculations. For the NEO calculations, only the hydrogen nucleus was treated quantum mechanically, and it was represented by a single nuclear basis function center with the DZSPDN nuclear basis set (i.e., 20 nuclear basis functions). The NEO-MP2 method was used to include both electron-electron and electron-proton correlation. The geometries were optimized at the NEO-MP2(ee) and NEO-MP2(ee+ep) levels. To include the X−X mode quantum effects in the NEO calculations, we implemented the NEO-MP2/1Dgrid approach. In this approach, the NEO-MP2 energy is calculated along a grid representing the X−X distances, and the Fourier grid Hamiltonian (FGH) method[37] is used to calculate the wave function corresponding to the X−X mode. The NEO-MP2/1Dgrid approach assumes an adiabatic separation between the hydrogen motion and the X−X motion (i.e., the hydrogen nucleus and the electrons are assumed to respond instantaneously to the motion of the heavy nuclei).

We emphasize that the NEO calculations are much faster than the two-dimensional grid and VSCF calculations. The two-dimensional potential energy surface used for the $[FHF]^-$ grid calculation of Del Bene and Jordan required 206 single point conventional MP2 energy calculations, and 1601 quadrature points were used to construct the VSCF potential. In contrast, only 32 NEO-MP2 calculations were used to construct the NEO-MP2/1Dgrid potential for $[FHF]^-$. For this system, a single NEO-MP2 energy calculation requires only ∼15 s of CPU time, which is similar to a conventional MP2 energy calculation.

Table 1 presents the X−X distances calculated with a number of different approaches. The two-dimensional grid method includes the nuclear quantum effects of the hydrogen and the X−X modes, as well as the coupling between these modes. The

VSCF method includes the quantum effects of the two bending modes, in addition to the hydrogen stretch and X−X modes, and describes the couplings among the modes in an approximate manner. The two-dimensional grid and VSCF methods do not include the response of the electronic wave function to the nuclear wave function or a rigorous treatment of electron-proton correlation because the nuclear wave functions are calculated on a Born-Oppenheimer electronic potential energy surface. In contrast, the quantum nuclear and electronic wave functions are calculated self-consistently in the NEO approach, and the NEO-MP2(ee+ep) method includes a significant amount of electron-proton dynamical correlation. The NEO-MP2(ee) and NEO-MP2(ee+ep) methods include the nuclear quantum effects of the hydrogen but not the X−X motion, whereas the NEO-MP2(ee)/1Dgrid and NEO-MP2(ee+ep)/1Dgrid methods include the nuclear quantum effects of the hydrogen and the X−X motions but not the coupling between these motions.

The NEO approach is capable of including the nuclear quantum effects of the bending mode with an adequate nuclear basis set, sufficient electron-proton correlation, and inclusion of nonadiabatic effects between the classical and quantum nuclei. The present implementation is aimed at an accurate description of the stretching modes, however, so the nuclear basis set is not optimized for the description of the lower-frequency bending modes. Inclusion of electron-proton correlation at the NEO-MP2(ee+ep) level provides an approximate description of these bending modes within the context of this nuclear basis set and in the absence of nonadiabatic effects between the classical and quantum nuclei.

The results provided in Table 1 indicate that inclusion of the nuclear quantum effects of the hydrogen significantly increases the X−X distance relative to the conventional MP2 method. Comparison of the NEO-MP2 and NEO-MP2/1Dgrid results illustrates that the quantum effects of the X−X motion are not as significant as those of the hydrogen motion. Specifically, the X−X distance is altered by nearly an order of magnitude more by the quantum effects of the hydrogen nucleus than by the quantum effects of the heavy nuclei. The NEO-MP2(ee)/1Dgrid method leads to an X−X distance within 0.001 Å of the distance obtained with the two-dimensional grid method for X = F and X = Cl. This excellent agreement provides validation for the NEO approach.

Analysis of the results for the three different halides indicates that the difference between the NEO-MP2(ee)/1Dgrid and the two-dimensional grid X−X distances is significantly greater for X = Br than for X = F and Cl. To verify that the hydrogen nuclear basis set is not the source of the discrepancies, we optimized the exponents in the nuclear basis functions for each system and found that the results did not change significantly. A source of error in the NEO-MP2/1Dgrid calculations is the adiabatic separation of the H and X−X motions. This error is expected to decrease as the mass of X increases. A source of error in the two-dimensional grid calculations of Del Bene and Jordan is the neglect of the impact of the nuclear wave functions on the electronic structure. This error is expected to increase as the number of electrons in X increases and is most likely responsible for the discrepancies when X = Br.

Inclusion of electron-proton dynamical correlation in the NEO calculations decreases the X−X distances by ∼0.01 Å. Similarly, the X−X distances calculated with the VSCF method are ∼0.01 Å shorter than the distances calculated with the two-dimensional grid method. The smaller X−X distances for the VSCF calculations are most likely due to the inclusion of the bending motions. As discussed above, the inclusion of electron-proton dynamical correlation improves the description of the bending modes within the NEO approach. An improved description of the bending modes through either VSCF or NEO-MP2(ee+ep) leads to better agreement of the calculated distances with the experimental R_0 values.[38,39]

TABLE 2: Experimental and Theoretical Symmetric Stretch Mode Frequencies in cm^{-1} for [XHX]$^-$ with X = F, Cl, Br

method	[FHF]$^-$	[ClHCl]$^-$	[BrHBr]$^-$
experiment	583[a]	318[b]	N/A
MP2-harmonic	633	345	208
2D grid[c]	589	317	195
VSCF-MP2	618	343	205
CC-VSCF-MP2	591	327	197
NEO-MP2(ee)/1Dgrid	606	334	212
NEO-MP2(ee+ep)/1Dgrid	611	334	206

[a] Reference 38. [b] Reference 39. [c] Reference 27.

The agreement between the NEO-MP2(ee+ep)/1Dgrid method and the experimental R_0 values provides further validation for the NEO approach. For X = F, the X−X distances obtained from the NEO-MP2(ee+ep)/1Dgrid and VSCF methods are ∼0.02 Å above the experimental R_0 value. The differences between the X−X distance obtained with the conventional MP2 method and the experimental R_e suggest that the remaining discrepancies may be due in part to limitations of the electronic basis set and level of electron correlation. Another potential source of error for the VSCF calculations is the approximate treatment of the couplings among the vibrational modes. A possible source of the discrepancy for the NEO calculations is the limited treatment of the bending modes due to the choice of nuclear basis set and level of electron-proton correlation. An additional source of error in the NEO approach is the adiabatic separation of the hydrogen and heavy atom motions. This error decreases as the mass of X increases. For [ClHCl]$^-$, the difference between the experimental R_0 value and the NEO-MP2(ee+ep)/1Dgrid distance decreases to 0.005 Å.

The frequencies corresponding to the X−X symmetric stretch mode are presented in Table 2. The conventional MP2 frequencies are significantly greater than the experimental values due to the neglect of anharmonic effects. The two-dimensional grid and CC-VSCF frequencies are much closer to the experimental values. The VSCF frequencies are greater than the CC-VSCF frequencies due to the lack of dynamical correlation among the vibrational modes in VSCF. The NEO-MP2/1Dgrid frequencies are smaller than the conventional MP2 frequencies but larger than the two-dimensional grid and CC-VSCF frequencies. The larger errors in the X−X symmetric stretch frequencies calculated with the NEO approach compared to those calculated with the two-dimensional grid and CC-VSCF methods are most likely due to a combination of the adiabatic separation of the hydrogen and X−X motions and an inadequate nuclear basis set in the outer regions of the NEO potential energy surfaces (i.e., for large X−X distances). The potential along the proton coordinate becomes a double well at large X−X distances. As shown in ref 21, an additional nuclear basis function center may be required for an accurate description of these types of potentials. The inclusion of an additional nuclear basis function center is expected to decrease the energy in the outer region of the potential energy surface along the X−X mode and thereby lead to a lower frequency for this mode. Although these types of calculations are straightforward, the level of accuracy provided in Table 2 is satisfactory for the purposes of this paper.

The asymmetric stretch and bending mode frequencies for the bihalides are given in Table 3. Note that the stretching and bending mode frequencies are of similar magnitude for the

TABLE 3: Experimental and Theoretical Bending (ν_2) and Asymmetric Stretch (ν_3) Mode Frequencies in cm^{-1} for $[XHX]^-$ with X = F, Cl, Br

	$[FHF]^-$		$[ClHCl]^-$		$[BrHBr]^-$	
method	ν_2	ν_3	ν_2	ν_3	ν_2	ν_3
experiment	1286[a]	1331[a]	N/A	723[b]	N/A	646[c]
MP2- harmonic	1334	1280	843	629	725	663
2D grid[d]	N/A	1485	N/A	881	N/A	846
VSCF-MP2	1283	1485	816	939	701	901
CC-VSCF-MP2	1277	1464	811	925	698	894

[a] Reference 38. [b] Reference 39. [c] Reference 43. [d] Reference 27.

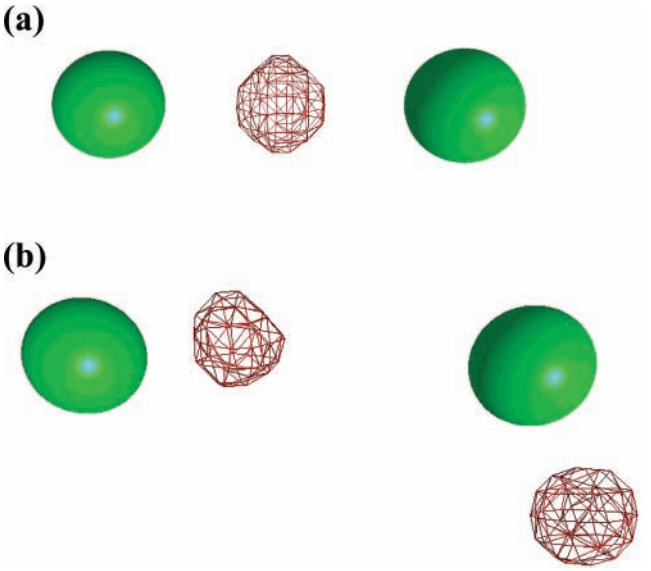

Figure 1. Depiction of (a) the bifluoride $[FHF]^-$ molecule and (b) the hydrogen fluoride (HF) dimer. The hydrogen nuclei are represented by nuclear wave functions computed with the NEO approach. The figures were generated using MacMolPlot[44] using a contour value of 0.05 au.

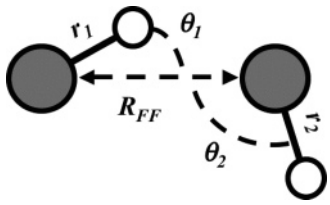

Figure 2. Definitions of the structural parameters for the HF dimer.

bihalides. The bending mode frequencies for $[FHF]^-$ calculated with the VSCF and CC-VSCF methods are in excellent agreement with the experimental value. The asymmetric stretch mode frequencies calculated with the VSCF and two-dimensional grid[27] methods are somewhat larger than the experimental values for all of the bihalides. The hydrogen stretching and bending mode frequencies are not calculated with the NEO-MP2 method because this method does not provide accurate excited vibronic states. Multiconfigurational NEO methods are being developed to enable the calculation of these frequencies.

B. Hydrogen Fluoride Dimer. In this subsection, we analyze calculations for the hydrogen fluoride (HF) dimer, which is depicted in Figure 2. The HF dimer is a prototypical hydrogen-bonded system for comparing electronic structure results to experimental structural and vibrational data.[40,41] In contrast to the $[XHX]^-$ systems, the hydrogen participating in the hydrogen bond in the HF dimer is not equally shared between the two fluorine atoms, and the potential for this hydrogen is highly asymmetric. Klemperer and co-workers have performed molecular beam experiments on this system.[28,29] They have calculated the F−F distance using a model that removes the large amplitude hydrogen bond exchange motion (i.e., the tunneling motions between equivalent hydrogen-bonded structures) but retains the stretching and bending motions about a single equilibrium geometry. Thus, the HF dimer is an ideal benchmark for the NEO, VSCF, and VPT2 approaches. In the NEO calculations for this system, both hydrogen nuclei were treated quantum mechanically.

TABLE 4: Experimental and Theoretical Structural Data for the HF Dimer[a]

method	R_{FF}	r_1	r_2	θ_1	θ_2
experiment[b]	2.72 ± 0.03[c] 2.7913[d]	N/A	N/A	10 ± 6[e]	117 ± 6[e]
RHF	2.830	0.903	0.902	6.77	119.70
MP2	2.746	0.928	0.925	6.37	111.15
CCSD(T)[f]	2.742	0.927	0.924	6.66	110.79
NEO-HF	2.787	0.925	0.922	6.29	119.76
NEO-MP2(ee)	2.717	0.931	0.928	6.53	110.92
NEO-MP2(ee+ep)	2.717	0.930	0.926	6.30	111.40
VSCF-MP2	2.772	0.926	0.928	6.92	111.78
VPT2-MP2	2.801	0.902	0.905	7.01	116.42

[a] Definitions for the structural parameters are given in Figure 2. Distances are in Å, and angles are in degrees. The aug-cc-pVTZ electronic basis set was used in all calculations. The DZSPDN nuclear basis set was used in all of the NEO calculations. Distances and angles involving the hydrogen nuclei were computed as expectation values with respect to the NEO hydrogen nuclear wave functions. [b] Reference 29. [c] The large amplitude bending motions are removed. [d] The stretching and bending motions are included. [e] In ref 29, these angles are interpreted to be associated with the equilibrium geometry. [f] Reference 41.

Table 4 provides the HF dimer F−F distances determined from conventional electronic structure methods, the VSCF and VPT2 methods, the NEO approach, and experimental data. The conventional RHF, MP2, and CCSD(T) calculations indicate that the F−F distance decreases as the amount of electron-electron correlation is increased. The NEO-HF calculation suggests that the F−F distance is also reduced when nuclear quantum effects are included. The impact of nuclear quantum effects on the F−F distance is on the same order as the impact of electron-electron correlation on this distance. When both electron-electron correlation and nuclear quantum effects are included in the NEO-MP2(ee) calculation, the F−F distance is further reduced. The NEO-MP2(ee) result illustrates that nuclear quantum effects and electron-electron correlation effects on the F−F distance are approximately additive for this system. Furthermore, when only the hydrogen-bonded hydrogen nucleus is treated quantum mechanically, the F−F distance is 2.733 Å with the reference Hamiltonian in eq 7 and 2.730 Å with the reference Hamiltonian in eq 2. Thus, relative to the CCSD(T) calculations, the nuclear quantum effects due to the terminal hydrogen in the HF dimer have the same impact on the F−F distance as those due to the hydrogen-bonding hydrogen.

As given in Table 4, the NEO-MP2(ee+ep) and NEO-MP2(ee) calculations yield the same F−F distance for the HF dimer. This observation indicates that electron-proton correlation is not significant with this nuclear basis set for this system. In contrast, for the $[XHX]^-$ systems discussed in the previous subsection, electron-proton correlation significantly altered the X−X distances with this nuclear basis set. Note that the reference Hamiltonian in eq 7 was used for the bihalide systems, which include only a single quantum nucleus, whereas the reference Hamiltonian in eq 2 was used for the HF dimer, which includes two quantum nuclei. We verified that the impact of electron-proton correlation on the X−X distances in the

TABLE 5: Experimental and Theoretical Vibrational Frequencies in cm^{-1} for the HF Dimer[a]

mode	experiment[b]	VPT2	CC-VSCF	VSCF	harmonic
stretch	3931	3916	3865	3866	4082
stretch	3868	3846	3802	3744	3989
bend	N/A	456	711	743	578
o/*p* bend	400	406	648	690	474
bend	394	153	559	568	219
F−F stretch	125, 128	130	123	227	159

[a] The theoretical frequencies were calculated at the MP2/aug-cc-pVTZ level. [b] Reference 40.

bihalides is still significant when the reference Hamiltonian in eq 2 is used. Thus, the greater impact of electron-proton correlation on the bihalides than on the HF dimer is not due to the different reference Hamiltonians but rather is due to the different types of proton potentials. The proton potentials for the bihalides are flat, symmetric single wells, whereas the proton potential for the HF dimer is a tighter, asymmetric single well along the donor-acceptor axis. Electron-proton correlation is more important for the bihalides because the proton nuclear wave function is more delocalized along the donor-acceptor axis. As discussed below, however, electron-proton correlation may be important for calculations of the HF dimer with a nuclear basis set designed to describe the lower frequency bending modes.

In addition to the F−F distance, the two angles and the H−F bond lengths defined in Figure 2 are also provided in Table 4. For the NEO approach, these quantities were calculated as expectation values with respect to the nuclear wave functions. The H−F bond lengths for both HF molecules increase when electron-electron correlation and nuclear quantum effects are included. The increase in the H−F bond lengths due to electron-electron correlation is of similar order as the increase due to nuclear quantum effects. The increased H−F distances result in larger dipole moments in each of the interacting HF molecules, thereby enhancing the electrostatic interaction between the HF monomers and decreasing the F−F distance. Thus, inclusion of nuclear quantum effects using the NEO approach strengthens the hydrogen bond in the HF dimer.

In contrast to the NEO-MP2 results, the F−F distances calculated with the VSCF and VPT2 methods are larger than the conventional electronic structure F−F distance. To evaluate the accuracy of the VSCF and VPT2 approaches for this system, we analyzed the vibrational frequencies calculated at the VSCF, CC-VSCF, and VPT2 levels. These frequencies are provided in Table 5. The frequencies calculated at the CC-VSCF and VPT2 levels are in reasonable agreement with the experimental frequencies compiled by Collins and co-workers.[40] The frequencies calculated at the VSCF level do not agree as well with these experimental frequencies. These discrepancies are most likely due to the omission of some important higher order terms in the implementation of VSCF in the GAMESS package.[8] As a result, the vibrationally averaged geometries calculated with the VPT2 method are expected to be more reliable than those calculated with this VSCF method.

The qualitative difference between the NEO results and the VSCF and VPT2 results for the F−F distance arises from the treatments of the bending-type modes. Previous studies[42] have suggested that librational motions in the water dimer increase the O−O distance. An analogous effect is expected to be observed in the HF dimer. As the separation between the two HF monomers is decreased slightly from equilibrium, the bending motions become more confined, increasing the zero point energy of these modes. In contrast, the stretching potential

TABLE 6: Experimental and Theoretical Structural Data for the DF Dimer[a]

method	R_{FF}	r_1	r_2	θ_1	θ_2
experiment[b]	2.778[c]	N/A	N/A	N/A	N/A
VSCF-MP2	2.765	0.924	0.925	6.75	111.55
VPT2-MP2	2.794	0.909	0.910	6.79	115.03

[a] Definitions for the structural parameters are given in Figure 1. Distances are in Å, and angles are in deg. The aug-cc-pVTZ electronic basis set was used in all calculations. [b] Reference 40. [c] The stretching and bending motions are included.

TABLE 7: Theoretical Vibrational Frequencies in cm^{-1} for the DF Dimer at the MP2/aug-cc-pVTZ Level

mode	VPT2	CC-VSCF	VSCF	harmonic
stretch	2872	2831	2839	2958
stretch	2818	2782	2758	2892
bend	354	502	519	417
o/*p* bend	306	429	463	341
bend	153	51	305	180
F−F stretch	114	79	296	137

of the shared hydrogen becomes flatter, reducing the zero point energy of this mode. The vibrationally averaged F−F distance is determined by a balance between the opposing effects of the stretching and bending modes, as well as the electrostatic effects. The VPT2 F−F distance of 2.801 Å is in excellent agreement with the vibrationally averaged F−F distance of 2.7913 Å determined experimentally by Klemperer and co-workers[29] for a model that includes all stretching and bending motions about a single equilibrium structure. The F−F distance of 2.717 Å calculated with the NEO-MP2 method is in excellent agreement with the distance of 2.72 Å obtained experimentally from a model that removes the large amplitude bending motions.[29]

We also studied the impact of isotopic substitution on the geometry of the HF dimer. Specifically, we calculated the F−F distance for the HF and DF dimers using the NEO-MP2, VSCF, and VPT2 approaches. The structural data for the DF dimer are presented in Table 6, and the calculated vibrational frequencies are presented in Table 7. For the NEO-MP2 calculations of the DF dimer, the DZSPDN(D) basis set optimized for deuterium[22] was used. The NEO-MP2(ee) F−F distance in the DF dimer was calculated to be 2.726 Å, which is ∼0.01 Å longer than the NEO-MP2(ee) distance for the HF dimer. As discussed in ref 22, this weakening of the hydrogen bond upon deuteration arises from the decrease in the H−F bond lengths and therefore the dipole moments of the HF monomers. Conversely, the VPT2 F−F distance in the DF dimer was calculated to be ∼0.01 Å shorter than the VPT2 distance for the HF dimer. A similar trend was found with the VSCF method. This decrease in the F−F distance by ∼0.01 Å upon deuteration was also observed experimentally by Klemperer and co-workers[29] for the model that includes all stretching and bending motions about a single equilibrium structure.

These results suggest that the NEO-MP2 calculations accurately account for the stretching motions of the hydrogen atoms but may not adequately describe the bending motions, which significantly impact the F−F distance for the HF dimer. The bending modes have a greater structural impact on the HF dimer than on the bihalides because the HF dimer bending modes have lower frequencies. Moreover, the stretching and bending frequencies in the HF dimer differ by an order of magnitude, whereas the stretching and bending frequencies in the bihalides are of similar magnitudes. The DZSPDN nuclear basis set was designed for higher-frequency stretching motions.[16] Thus, the DZSPDN basis set adequately describes the hydrogen vibrational ground state in the bihalide systems, but it may not

give the correct hydrogen vibrational ground state in the HF dimer due to the significant difference between the bending and stretching frequencies. We performed NEO-MP2 calculations on the hydrogen fluoride dimer with a larger nuclear basis set (i.e., quadruple-ζ *s* and *p* and double-ζ *d*) with frequencies ranging from 400 to 4000 cm^{-1}, and the results were virtually identical to those obtained with the DZSPDN nuclear basis set. We also found that including proton-proton correlation at the NEO-full CI level[16,19] did not alter the qualitative trends. These results suggest that additional electron-proton dynamical correlation or multiconfigurational nuclear-electronic wave functions[16,19] may be required to accurately predict geometries for these types of systems. Note that these large amplitude bending motions will be damped in large clusters and condensed phase environments. The path integral Car-Parrinello molecular dynamics results of Raugei and Klein for liquid HF indicate that inclusion of nuclear quantum effects decreases the F−F distance in solution.[14]

IV. Conclusions

We have investigated the structural impact of nuclear quantum effects for a set of bihalides, $[XHX]^-$ with X = F, Cl, Br, and the hydrogen fluoride dimer. These two types of hydrogen bonding systems are fundamentally different because the proton potential along the donor-acceptor axis is flat and symmetric for the bihalides but tighter and asymmetric for the HF dimer. Moreover, the difference between the bending and stretching mode frequencies is significantly greater for the HF dimer than for the bihalides. We compared structural parameters obtained from conventional electronic structure methods, multidimensional grid methods, the VSCF and VPT2 methods, the NEO-MP2 approach, and experimental data. Our analysis provides insight into key physical principles governing the structural properties of hydrogen-bonded systems.

For the bihalides $[XHX]^-$, inclusion of the nuclear quantum effects of the hydrogen significantly increases the X−X distance. The quantum effects of the hydrogen motion impact the X−X distance by nearly an order of magnitude more than the quantum effects of the X−X motion. The X−X distances calculated with the NEO-MP2(ee)/1Dgrid method are in excellent agreement with the distances calculated with the Born-Oppenheimer two-dimensional grid method.[27] The differences between the X−X distances calculated with these two methods are only ∼0.001 Å for X = F and Cl. The slightly larger discrepancies for X = Br are most likely due to the neglect of the impact of the nuclear wave functions on the electronic structure in the two-dimensional grid method. The NEO-MP2(ee+ep) and VSCF methods lead to smaller X−X distances that are in better agreement with the experimental R_0 values available for X = F and Cl. This improvement is due to a more accurate description of the bending modes, which are neglected in the two-dimensional grid method. The difference between the NEO-MP2(ee+ep)/1Dgrid and experimental X−X distances is only ∼0.005 Å for X = Cl. This agreement is slightly better for X = Cl than for X = F because the adiabatic separation between the hydrogen and heavy atom motions is a more valid approximation for X = Cl.

The HF dimer is a more challenging system for these approaches because it exhibits bending motions that have much lower frequencies than the stretching motions. Inclusion of the hydrogen quantum effects using the NEO-MP2 approach decreases the F−F distance in the HF dimer. The physical basis for this observation is that the H−F bond lengths of both HF molecules increase when nuclear quantum effects are included, resulting in larger dipole moments in each molecule and therefore a stronger electrostatic interaction between the HF monomers. The NEO-MP2 F−F distance of 2.717 Å is in excellent agreement with the distance of 2.72 Å obtained experimentally for a model that removes the large amplitude bending motions.[29] These results illustrate that the NEO-MP2 approach accurately describes the stretching motions. In contrast to the NEO-MP2 results, the inclusion of nuclear quantum effects with the VSCF and VPT2 methods increases the F−F distance. The VPT2 F−F distance of 2.802 Å is in excellent agreement with the distance of 2.7913 Å obtained experimentally with a model that includes all stretching and bending motions around a single equilibrium structure.[29] For the isotopically substituted DF dimer, the VPT2 method predicts a decrease in the F−F distance by ∼0.01 Å. This decrease in the F−F distance upon deuteration is consistent with the experimental data.[29] These results indicate that the VPT2 method accurately describes both the stretching and the low-frequency bending motions.

Our analysis provides a comprehensive evaluation of the applicability of the NEO approach to the investigation of hydrogen-bonded systems. The agreement of the NEO-MP2 calculations with multidimensional grid, VSCF, and VPT2 calculations, as well as experimental data, illustrates the potential of the NEO approach for calculating quantitatively accurate structures. The NEO approach is substantially more efficient than the multidimensional grid, VSCF, and VPT2 methods and therefore will enable the inclusion of nuclear quantum effects for much larger systems. In large clusters and condensed phase environments, the low-frequency bending modes are not expected to impact the geometries as significantly. Future work will focus on the extension of the NEO approach to describe low-frequency bending motions more accurately. These extensions will involve the development of more flexible nuclear basis sets and methods that include additional electron-proton correlation and nonadiabatic couplings between the hydrogen and heavy atom motions.

Acknowledgment. We gratefully acknowledge the support of AFOSR Grant No. FA9550-04-1-0062 and NIH Grant GM56207. We also wish to thank Mike Pak and Jonathan Skone for helpful discussions and Ken Jordan and Kadir Diri for assistance with the VPT2 calculations.

References and Notes

(1) Brooks, C. L., III; Karplus, M. *Adv. Chem. Phys.* **1988**, *71*, 1.
(2) Moriuchi, T.; Tamura, T.; Hirao, T. *J. Am. Chem. Soc.* **2002**, *124*, 9356.
(3) Finney, J. L. *Faraday Discuss.* **1996**, *103*, 1.
(4) Headrick, J. M.; Bopp, J. C.; Johnson, M. A. *J. Chem. Phys.* **2005**, *121*, 11523.
(5) Hammer, N. I.; Diken, E. G.; Roscioli, J. R.; Johnson, M. A.; Myshakin, E. M.; Jordan, K. D.; McCoy, A. B.; Huang, X.; Bowman, J. M.; Carter, S. *J. Chem. Phys.* **2005**, *122*, 244301.
(6) Gregory, J. K.; Clary, D. C. *J. Phys. Chem.* **1996**, *100*, 18014.
(7) Clary, D. C.; Benoit, D. M.; van Mourik, T. *Acc. Chem. Res.* **2000**, *33*, 441.
(8) Chaban, G. M.; Jung, J. O.; Gerber, R. B. *J. Chem. Phys.* **1999**, *111*, 1823.
(9) Bowman, J. M. *Acc. Chem. Res.* **1986**, *19*, 202.
(10) Carter, S.; Bowman, J. M.; Handy, N. C. *Theor. Chem. Acc.* **1998**, *100*, 191.
(11) Barone, V. *J. Chem. Phys.* **2005**, *122*, 014108.
(12) Diri, K.; Myshakin, E. M.; Jordan, K. D. *J. Phys. Chem. A* **2005**, *109*, 4005.
(13) Tuckerman, M. E.; Marx, D.; Klein, M. L.; Parrinello, M. *J. Chem. Phys.* **1996**, *104*, 5579.
(14) Raugei, S.; Klein, M. L. *J. Am. Chem. Soc.* **2003**, *125*, 8992.
(15) Chen, B.; Ivanov, I.; Klein, M. L.; Parrinello, M. *Phys. Rev. Lett.* **2003**, *91*, 215503.

(16) Webb, S. P.; Iordanov, T.; Hammes-Schiffer, S. *J. Chem. Phys.* **2002**, *117*, 4106.
(17) Iordanov, T.; Hammes-Schiffer, S. *J. Chem. Phys.* **2003**, *118*, 9489.
(18) Pak, M. V.; Hammes-Schiffer, S. *Phys. Rev. Lett.* **2004**, *92*, 103002.
(19) Pak, M. V.; Swalina, C.; Webb, S. P.; Hammes-Schiffer, S. *Chem. Phys.* **2004**, *304*, 227.
(20) Swalina, C.; Pak, M. V.; Hammes-Schiffer, S. *Chem. Phys. Lett.* **2005**, *404*, 394.
(21) Swalina, C.; Pak, M. V.; Hammes-Schiffer, S. *J. Chem. Phys.* **2005**, *123*, 014303.
(22) Reyes, A.; Pak, M. V.; Hammes-Schiffer, S. *J. Chem. Phys.* **2005**, *123*, 064104.
(23) Tachikawa, M.; Mori, K.; Osamura, Y. *Mol. Phys.* **1999**, *96*, 1207.
(24) Tachikawa, M. *Mol. Phys.* **2002**, *100*, 881.
(25) Udagawa, T.; Ishimoto, T.; Tokiwa, H.; Tachikawa, M.; Nagashima, U. *Chem. Phys. Lett.* **2004**, *389*, 236.
(26) Shibl, M. F.; Tachikawa, M.; Kuhn, O. *Phys. Chem. Chem. Phys.* **2005**, *7*, 1368.
(27) Del Bene, J.; Jordan, M. *Spectrochim. Acta, Part A* **1999**, *55*, 719.
(28) Dyke, T. R.; Howard, B. J.; Klemperer, W. J. *J. Chem. Phys.* **1972**, *56*, 2442.
(29) Howard, B. J.; Dyke, T. R.; Klemperer, W. J. *J. Chem. Phys.* **1984**, *81*, 5417.
(30) Schmidt, M. W.; Baldridge, K. K.; Boatz, J. A.; Elbert, S. T.; Gordon, M. S.; Jensen, J. H.; Koseki, S.; Matsunaga, N.; Nguyen, K. A.; Su, S.; Windus, T. L.; Dupuis, M.; Montgomery, J. A. *J. Comput. Chem.* **1993**, *14*, 1347.
(31) Dunning, T. H., Jr. *J. Chem. Phys.* **1989**, *90*, 1007.
(32) Woon, D. E.; Dunning, T. H., Jr. *J. Chem. Phys.* **1993**, *98*, 1358.
(33) Woon, D. E.; Dunning, T. H., Jr. *J. Chem. Phys.* **1994**, *100*, 2975.
(34) Simon, S.; Duran, M.; Dannenberg, J. J. *J. Chem. Phys.* **1996**, *105*, 11024.
(35) Boys, S. F.; Bernardi, F. *Mol. Phys.* **1970**, *19*, 553.
(36) Frisch, M. J.; Trucks, G. W.; Schlegel, H. B.; Scuseria, G. E.; Robb, M. A.; Cheeseman, J. R.; Montgomery, J. A., Jr.; Vreven, T.; Kudin, K. N.; Burant, J. C.; Millam, J. M.; Iyengar, S. S.; Tomasi, J.; Barone, V.; Mennucci, B.; Cossi, M.; Scalmani, G.; Rega, N.; Petersson, G. A.; Nakatsuji, H.; Hada, M.; Ehara, M.; Toyota, K.; Fukuda, R.; Hasegawa, J.; Ishida, M.; Nakajima, T.; Honda, Y.; Kitao, O.; Nakai, H.; Klene, M.; Li, X.; Knox, J. E.; Hratchian, H. P.; Cross, J. B.; Adamo, C.; Jaramillo, J.; Gomperts, R.; Stratmann, R. E.; Yazyev, O.; Austin, A. J.; Cammi, R.; Pomelli, C.; Ochterski, J. W.; Ayala, P. Y.; Morokuma, K.; Voth, G. A.; Salvador, P.; Dannenberg, J. J.; Zakrzewski, V. G.; Dapprich, S.; Daniels, A. D.; Strain, M. C.; Farkas, O.; Malick, D. K.; Rabuck, A. D.; Raghavachari, K.; Foresman, J. B.; Ortiz, J. V.; Cui, Q.; Baboul, A. G.; Clifford, S.; Cioslowski, J.; Stefanov, B. B.; Liu, G.; Liashenko, A.; Piskorz, P.; Komaromi, I.; Martin, R. L.; Fox, D. J.; Keith, T.; Al-Laham, M. A.; Peng, C. Y.; Nanayakkara, A.; Challacombe, M.; Gill, P. M. W.; Johnson, B.; Chen, W.; Wong, M. W.; Gonzalez, C.; Pople, J. A. Gaussian 03. Gaussian, Inc.: Pittsburgh, PA, 2003.
(37) Marston, C. C.; Balint-Kurti, G. G. *J. Chem. Phys.* **1989**, *91*, 3571.
(38) Kawaguchi, K.; Hirota, E. *J. Chem. Phys.* **1987**, *87*, 6838.
(39) Kawaguchi, K. *J. Chem. Phys.* **1988**, *88*, 4186.
(40) Collins, C. L.; Morihashi, K.; Yamaguchi, Y.; Schaefer, H. F., III. *J. Chem. Phys.* **1995**, *103*, 6051.
(41) Peterson, K. A.; Dunning, T. H., Jr. *J. Chem. Phys.* **1995**, *102*, 2032.
(42) Astrand, P.-O.; Karlstrom, G.; Engdahl, A.; Nelander, B. *J. Chem. Phys.* **1995**, *102*, 3534.
(43) Rasanen, M.; Seetula, J.; Kunttu, H. *J. Chem. Phys.* **1993**, *98*, 3914.
(44) Bode, B. M.; Gordon, M. S. *J. Mol. Graphics* **1998**, *16*, 133.